The thermal metal-insulator phase transition in (EDO-TTF)(2)PF6

Linker, Gerrit-Jan; van Duijnen, Piet Th.; van Loosdrecht, Paul H. M.; Broer, Ria

Published in:
Molecular Physics

DOI:
10.1080/00268976.2016.1263765

Publication date:
2017

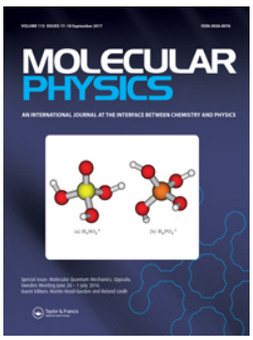

Taylor & Francis
Taylor & Francis Group

Molecular Physics

An International Journal at the Interface Between Chemistry and Physics

ISSN: 0026-8976 (Print) 1362-3028 (Online) Journal homepage: https://www.tandfonline.com/loi/tmph20

The thermal metal-insulator phase transition in $(EDO\text{-}TTF)_2PF_6$

Gerrit-Jan Linker, Piet Th. van Duijnen, Paul H. M. van Loosdrecht & Ria Broer

To cite this article: Gerrit-Jan Linker, Piet Th. van Duijnen, Paul H. M. van Loosdrecht & Ria Broer (2017) The thermal metal-insulator phase transition in $(EDO\text{-}TTF)_2PF_6$, Molecular Physics, 115:17-18, 2180-2184, DOI: 10.1080/00268976.2016.1263765

To link to this article: https://doi.org/10.1080/00268976.2016.1263765

Published online: 06 Dec 2016.

MOLECULAR PHYSICS, 2017
VOL. 115, NOS. 17-18, 2180–2184
http://dx.doi.org/10.1080/00268976.2016.1263765

Taylor & Francis
Taylor & Francis Group

MQM 2016

The thermal metal-insulator phase transition in $(EDO\text{-}TTF)_2PF_6$

Gerrit-Jan Linker[a], Piet Th. van Duijnen[b], Paul H. M. van Loosdrecht[c] and Ria Broer[a]

[a]Department of Theoretical Chemistry, Zernike Institute for Advanced Materials, University of Groningen, Groningen, The Netherlands; [b]Stichting Moleculaire Quantum Mechanica, Leek, The Netherlands; [c]Physics Institute 2, University of Cologne, Cologne, Germany

ABSTRACT

The thermal metal-insulator phase transition in the π-stacked $(EDO\text{-}TTF)_2PF_6$ charge transfer salt is of the Peierls type. It is related to geometrical reorganisations and charge ordering phenomena. We report that dimerising displacements are involved in the mechanism of this transition. By using periodic quantum chemical calculations, we find a double well potential in which dimerisation and charge localisation become manifest. By analysing the nuclear wavefunctions we discuss the mechanism of the phase transition in terms of thermal fluctuations.

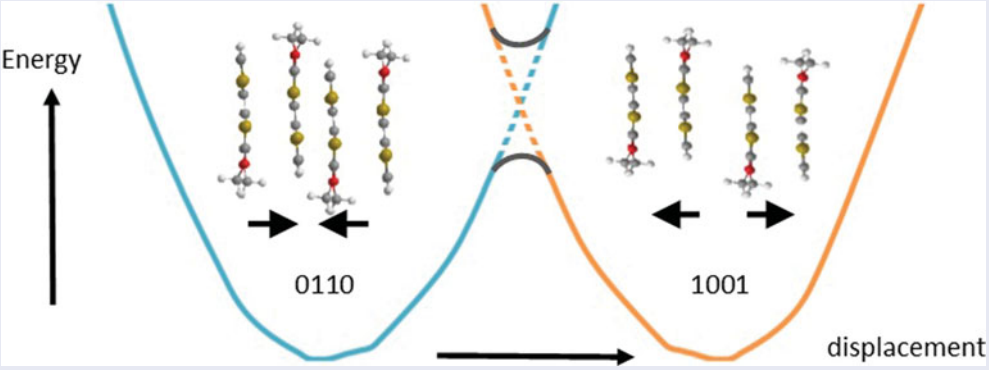

ARTICLE HISTORY
Received 6 October 2016
Accepted 14 November 2016

KEYWORDS
$(EDO\text{-}TTF)_2PF_6$; phase transition; Peierls; dimerising displacement; double well potential

1. Introduction

$(EDO\text{-}TTF)_2PF_6$ is an organic charge transfer salt in which electrons are transferred from ethylenedioxy-tetrathiafulvalene (EDO-TTF) to PF_6 molecules. In the crystal, the near planar and flexible EDO-TTF molecules form columns in which the molecules weakly interact through the overlap of π-orbitals. Acceptor PF_6 molecules reside in between electron donor EDO-TTF columns. The interesting physics of the system is largely due to holes created in the EDO-TTF columns by the charge transfer process. $(EDO\text{-}TTF)_2PF_6$ has been reported to exhibit a first-order metal-insulator phase transition which is accompanied by geometrical reorganisations and charge ordering phenomena [1]. At temperatures above $T_{M-I} = 278$ K, the holes delocalise over equidistant EDO-TTF molecules in the columns. The conductivity in the high temperature (HT) phase is metallic: $\sigma_{300\ K} = 60$ S/cm [2]. There are two EDO-TTF molecules in the unit cell which have equal molecular charge of +½ and a planar geometry. The electronic band structure obtained from quantum chemical periodic calculations [3] shows that, in this phase, frontier bands are partially occupied confirming the good electrical conductivity. At lower temperatures, $(EDO\text{-}TTF)_2$ dimerisation is observed in which the holes order in a 0110 pattern (each digit represents the positive molecular EDO-TTF charge in a single stack tetramer unit cell). The conductivity in the low temperature (LT) phase is like that of an insulator: $\sigma_{260\ K} = 14$ μS/cm [2]. The band structure of the LT phase exhibits a band gap [3]. In this phase, there are four EDO-TTF molecules in the unit cell. Two neutral molecules have a boat (B) shape, and two positively charged molecules are planar (P). The tight relation between molecular charge and geometry, and also a rationalisation of the molecular geometries was established by us earlier [4,5]. The ordering of these molecules in the stack is BPPB (B and P denote a bent and planar molecular geometry respectively). The stacking of EDO-TTF molecules is not as regular as in the HT phase. This causes

CONTACT Gerrit-Jan Linker g.j.linker@oraxcel.com

a lowering of the band dispersion which leads to a separation in energies of the valence and conduction band.

The phase transition in $(EDO\text{-}TTF)_2PF_6$ is attributed to an interplay of instabilities that all have a structural origin [6]: molecular flexibility of EDO-TTF, geometrical ordering of EDO-TTF molecules associated to the charge ordering and an ordering of the PF_6 anions. From the analysis of frontier crystal orbitals [4], it was concluded that the phase transition is of the Peierls type. In the HT phase the conduction band, which is antibonding between dimers, is slightly populated whereas the bonding valence band is proportionally depopulated. The interaction between dimers is larger in the band gapped LT phase. Apparently, the symmetry lowering dimerising deformation is stabilising. Besides EDO-TTF dimerisation, PF_6 molecules also pair up in the LT phase and they show a restricted rotation [2]. In the HT phase, PF_6 molecules are equidistant in the stacking direction, and their rotation is isotropic. A conducting phase can also be achieved through a photo-induced phase transition [7,8,9].

In this paper, we report a rationalisation of the phase transition mechanism. We used quantum chemical methods to study the dimerising deformation of $(EDO\text{-}TTF)_2$ dimers in the HT X-ray crystal geometry. We established that the non-deformed system is bistable. In previous work we showed, from periodic spin-restricted Hartree-Fock (RHF) calculations in which the HT X-ray crystal geometry was used, that besides a state with delocalised holes, a 0110 charge ordered state could also be found. We now find that the charge-ordered state is stabilised by a dimerising displacement.

2. Computational details

We used the RHF method. Periodic calculations were performed, in which all electrons in the crystal were treated explicitly, and in which the HT X-ray crystal geometry [2] was used. The unit cell was doubled to contain a stack of four EDO-TTF molecules and two PF_6 molecules. The 6-21G basis set [10] and the Crystal software [11] were used. In our calculations, no local symmetry was imposed on the orbitals. We note that at this level of the theory it is not expected that energy profiles for intermolecular interactions can be calculated accurately, so we discuss our results qualitatively.

3. Periodic calculations for the dimerising $(EDO\text{-}TTF)_2$ displacement

We look for diabatic states crossing in energy upon making geometrical deformations. A good starting point for such a study is a standard vibrational analysis, however, a minimum energy conformation could not be obtained for the crystal. Instead, the displacement patterns of the molecules are based on simpler models. We assume that PF_6 molecules and EDO-TTF molecules form more or less separate entities in the $(EDO\text{-}TTF)_4(PF_6)_2$ crystal. PF_6 molecules are at relatively large distances from the EDO-TTF stacks and there is negligible contribution of PF_6 to the frontier crystal orbitals. We only consider displacements of initially equidistant, rigid EDO-TTF molecules in the tetramer unit cell. There are various displacement patterns along the stacking direction (Figure 1). In the 'dimer exchange' displacement Q_1, neighbour EDO-TTF molecules move pairwise toward or away from each other, leading to an exchange of the molecules that pair to form a dimer. The intermolecular distances change from all a to $a-2q$, $a+2q$, $a-2q$, etc. Displacement Q_2 gives a dimerised pattern, with intermolecular distances $a-2q$, a, $a+2q$, a, $a-2q$, etc. In the periodic calculations, displacement Q_3 is equivalent to Q_2 after a translation over ¼ of the unit cell length.

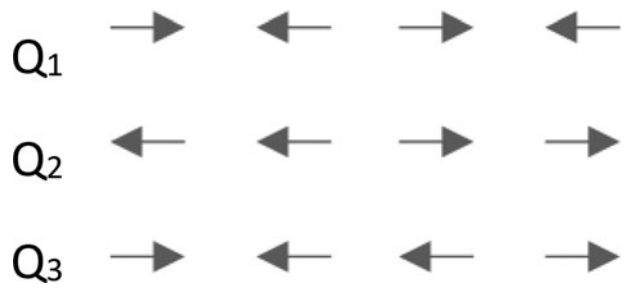

Figure 1. Unique longitudinal displacement patterns of molecules in a periodic chain of four identical particles.

The effect of EDO-TTF displacements Q_1, Q_2 and Q_3 is summarised in Figure 2. Periodic RHF calculations on the crystal are performed in which the EDO-TTF molecules are displaced according to the displacements in Figure 1, while the PF_6 molecules are fixed at their crystallographic positions. Crossing states are found only following the Q_2 dimerising $(EDO\text{-}TTF)_2$ displacement.

For the highest energy displacement, the dimer exchange displacement (Q_1), the total energy changes harmonically with a minimum at the equilibrium position. During the displacement, the charge ordering jumps abruptly between 1100 and 0110 at a displacement of −0.22 Å. Positive charge localises in one of two dimers. Movement of the molecules in the opposite direction causes the holes to localise in the dimer in the centre of the unit cell.

For the $(EDO\text{-}TTF)_2\cdots(EDO\text{-}TTF)_2$ dimerising displacement Q_2, three charge ordered solutions could be found using periodic RHF calculations. For displacement Q_2, the 0110 and 1001 charge ordered states could be followed separately. Despite the equivalent displacement

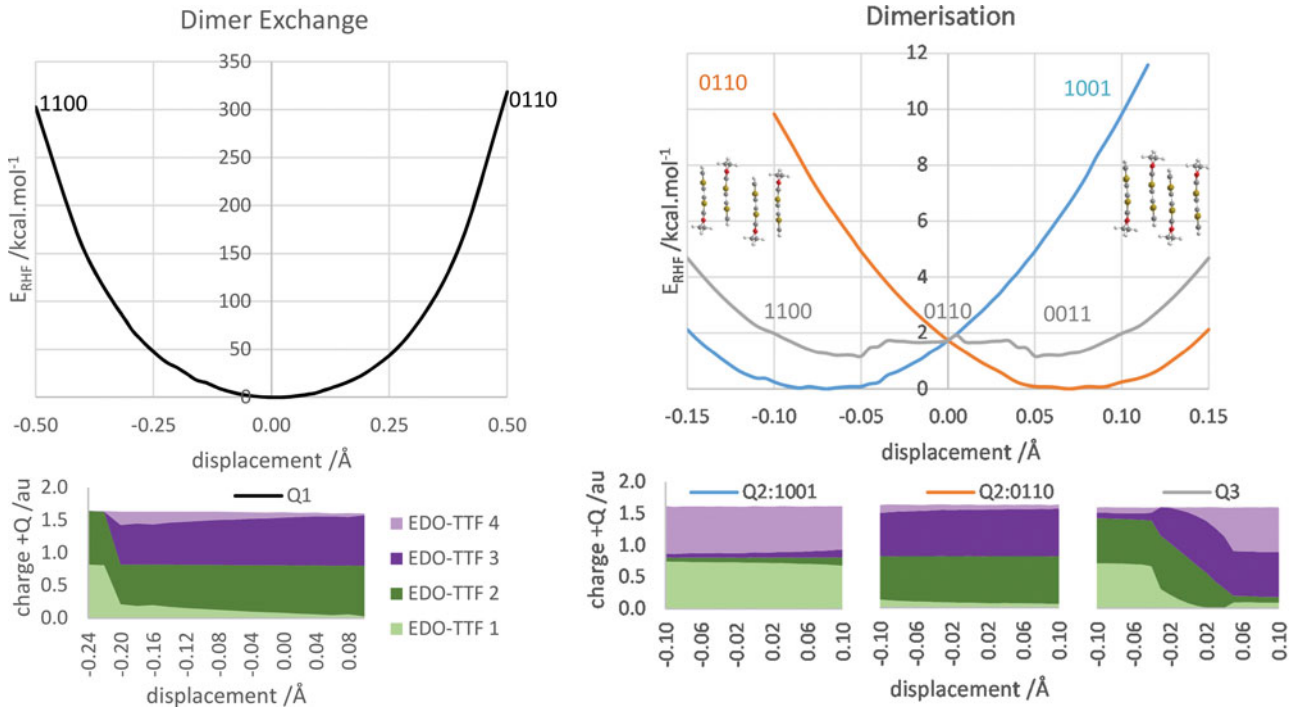

Figure 2. Total RHF energy vs. displacement for the dimer exchange displacement and the dimerising displacement (top) and the associated change in charge distribution (below) in the EDO-TTF tetramer stack. The ball-stick diagrams denote the $(EDO\text{-}TTF)_4$ geometry that corresponds to the displacement. The charge ordering patterns are indicated as 0110, 1001, 1100 or 0011.

pattern in Q_3, here the charge ordering changes gradually from 0011 through 0110 to 1100 and vice versa over a displacement of 0.1 Å. During these transitions the total energy changes within 1 kcal/mol. The lack of smoothness of the energy curves is likely due to choices of cut-off values in the Crystal software. At a point without geometrical distortion, the 0110 and 1001 states have the same relative energy of 1.7 kcal/mol (73 meV). Moving the $(EDO\text{-}TTF)_2$ dimers closer or separating them is equivalent due to the periodic boundary conditions. A double well energy curve is found with a minimum at a $(EDO\text{-}TTF)_2$ displacement of 0.065 Å. The distance between dimers at the minima is 0.13 Å less on one side and 0.13 Å more on the other side, compared to situation at zero displacement, where the EDO-TTF molecules are equidistant (at 3.67 Å). The minimum for Q_3 is for a displacement of ±0.05 Å. The energy of the 1100 and 0011 states is intermediate between 1001 and 0110.

The periodic calculations were checked in several ways. Qualitatively, the same results were obtained when integrals were calculated at higher precision (no expansions for the Coulomb integrals were used). The energy at the crossing point of the state becomes 1.4 kcal/mol (61 meV) while the minimum remains at a displacement of 0.065 Å. By using the 6-21G** basis set qualitatively the same results were obtained, thus ruling out basis set effects. Now, the crossing point of the states is at a relative energy of 1.9 kcal/mol (82 meV) while the minima are found for a displacement of 0.08 Å. The double minimum potential was also reproduced in periodic $m_s = 0$ spin-unrestricted Hartree-Fock (UHF) calculations in which the solutions have the 0110 charge ordering. In these calculations $E_x = 1.78$ kcal/mol (77 meV) with a minimum at about 0.07 Å. The total energy of these UHF solutions is 0.14 kcal/mol (5.9 meV) below the RHF solution at E_x and 0.18 kcal/mol (7.5 meV) at the minima. The UHF results indicate that there is no necessity to use a multi-determinantal approach to obtain the double minimum potential. Equivalent calculations were also performed with spin-restricted and spin-unrestricted DFT using the PBE0 functional [12]. In these calculations no bistable state was found, and a harmonic, single minimum, potential was obtained. The charge distribution changes a little from ½½½½ (non-displaced) in the direction of 0110/1001. At small displacements the system is a band-conductor while at displacements greater than 0.28 Å the band structure exhibits a valence-conduction band gap. While our RHF results fit well to the physics of the system, clearly with DFT(PBE0) charge localisation is not achieved by applying the Q_2 displacement.

To arrive at the adiabatic representation we need to calculate the interaction between the diabatic states.

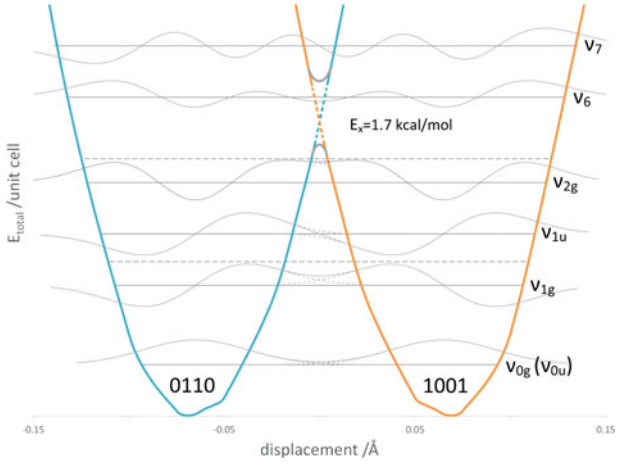

Figure 3. Representation of the 0110, 1001 state interaction, by depicted by dashing the RHF energies around E_x where also the adiabatic electronic energies are sketched. Horizontal lines indicate the vibrational levels. At energies below E_x, the levels for gerade and ungerade superpositions are split (solid lines). The nuclear wavefunctions sketched in the potential belong to the diabatic ground state potentials.

At the X-ray geometry (at zero displacement), the 0110 and 1001 states have the same electronic energy. We construct linear combinations of the diabatic electronic wavefunctions:

$$\Psi_{+/-} = (\Psi_a \pm \Psi_b) / \sqrt{(2 \pm 2S_{ab})} \tag{1}$$

where a and b denote the 0110 and 1001 wavefunctions, respectively, yielding two adiabatic wavefunctions Ψ_+ and Ψ_-. The splitting Δ between the adiabatic states, at zero displacement, can be calculated as follows:

$$\Delta = 2\,|H_{ab} - S_{ab}E_x| \,/\, \left(1 - S_{ab}^2\right) \tag{2}$$

In Equation (2), $H_{ab} = \Psi_a|\hat{H}|\Psi_b$, $S_{ab} = \Psi_a|\Psi_b$, and we used $H_{aa} = H_{bb} = E_x$. Here, H_{ab} is small due to the Slater–Condon rules: $H_{ab} = \cdots 0110\ 0110 \cdots |\hat{H}| \cdots 1001\ \ 1001 \cdots \approx 0$, in which a 1 (0) in the determinants indicates an (un)occupied localised EDO-TTF HOMO orbital. Due to a small overlap between the 0110 and 1001 states, $S_{ab} \neq 0$, we obtain two separated adiabatic electronic states. Around the crossing point, the adiabatic states are indicated in Figure 3 by full lines, the diabatic states by dashed lines.

We extend our analysis by explicitly considering nuclear motion. Whether the bistability of the system becomes manifest depends on the temperature and also on the height of the barrier. The zero-point energy for the 0110 (left) and 1001 (right) states is calculated as $\frac{1}{2}h\nu =$ 0.25 kcal/mol (11 meV), and it is shown as a horizontal line in the potential in Figure 3. In fact, below the crossing, which we calculated at $E_x = 1.7$ kcal/mol (74 meV), the nuclear wavefunctions of the system are superpositions:

$$\phi(q)_{+/-} = \left[\phi(q)_{\text{left}} \pm \phi(q)_{\text{right}}\right] \Big/ \sqrt{2\left(1 \pm S_{\text{left/right}}\right)} \tag{3}$$

(q denotes the displacement coordinate). The splitting of the corresponding energy levels depends on the overlap $S_{\text{left/right}} = \phi_{\text{left}}|\phi_{\text{right}}$. The overlap lowers the gerade combination but it raises the ungerade combination in energy more. In Figure 3, the uncoupled levels are dashed while the split levels are solid. For ν_0, the overlap $S_{\text{left/right}}$ is negligible: $S_{\text{left/right}} \approx 0$, and there is a negligible splitting in energy between ϕ_{0g} and ϕ_{0u} (ϕ_{0u} not shown). For ν_2, $S \neq 0$, and the energy of ϕ_{2u} is shifted to above E_x. Above E_x, the nuclear wavefunctions are determined by the walls of the potential on either side. For this wider potential, the quanta are smaller than it is the case for the two narrow potentials. Above E_x, there is less probability for the system to be found close to the barrier and we indicated that with a damped function. The effect of which is decreased for higher vibrational levels. At high enough energies the system can go to the excited adiabatic state.

4. Conclusions

The phase transition can be summarised as follows. Using a unit cell, with two EDO-TTF molecules, in previous work [13], we found an RHF state at $E = 4.7$ kcal/mol (204 meV). We regard this system as highly symmetric: all EDO-TTF molecules are equidistant and the charge ordering is ½½½½. This system is unstable to forming a 0110/1001 charge ordering, comparable to how Paldus and coworkers describe a similar instability of RHF solutions in cyclic polyenes [14]. They showed that the existence of a broken symmetry electronic wavefunction implies the tendency towards a distorted geometry. We observed a similar instability. Using a dimerised geometry we always find a charge ordered RHF electronic wavefunction. Only for a geometry with equidistant molecules we also find a higher symmetric solution with delocalised holes. The stabilisation of the charge ordered solution is due to the gain in induction energy. Induction energy increases quadratically with the electric field and therefore it is also quadratic with charge. The equidistant periodic system with a ½½½½ charge distribution has a smaller induction energy than the same system with a 0110 charge ordering. In Figure 3, we obtain a better representation of the system with a delocalised hole, compared to the highly symmetric RHF state.

At high temperatures, vibrational levels above E_x can become populated. The system has an average geometry with equidistant molecules. Just, above E_x, the probability to find the system in the middle of the potential is reduced due to the barrier. At these energies, the effect of the barrier is that the probability to find the system in one of the two dimerised geometries is increased. Below the barrier, the nuclear wavefunctions become superpositions of $\phi_{\text{left}}$and ϕ_{right}. At these temperatures, the electronic wavefunction fluctuates between a 0110 and 1001 charge ordering. Thereby it can be considered as symmetry broken. At lower temperatures and hence at lower energies, the left/right interchange is diminished due to the reduced amplitude of the nuclear wavefunction around zero displacement. The phase transition occurs when the interchange is significantly reduced, e.g. at ν_1. We calculate energies of 0.25 and 0.75 kcal/mol (11 and 33 meV) for ν_0 and ν_1, respectively, the difference of which is of the order of $k_B T_{M-\ I}$ (0.55 kcal/mol; 24 meV). At very low temperatures the system freezes into the 0110 or 1001 charge ordered states with a dimerised geometry. In previous work [3] we found these states to be band insulators.

Disclosure statement

No potential conflict of interest was reported by the authors.

References

[1] H. Yamochi and S-Y. Koshihara, Sci. Technol. Adv. Mater. **10**, 024305 (2009).
[2] A. Ota, H. Yamochi, and G. Saito, J. Mat. Chem. **12**, 2600 (2002).
[3] G.J. Linker, P.H.M. van Loosdrecht, P.Th. van Duijnen, and R. Broer, Phys. Chem. Chem. Phys. **17**, 30371 (2015).
[4] G.J. Linker, P.H.M. van Loosdrecht, P.Th. van Duijnen, and R. Broer, Chem. Phys. Lett. **487**, 220 (2010).
[5] G.J. Linker, P.Th. van Duijnen, P.H.M. van Loosdrecht, and R. Broer, J. Phys. Chem. A **116**, 7219 (2012).
[6] K. Saito, S. Ikeuchi, A. Ota, H. Yamochi, and G. Saito, Chem. Phys. Lett. **401**, 76 (2005).
[7] M. Chollet, L. Guerin, N. Uchida, S. Fukaya, H. Shimoda, T. Ishikawa, K. Matsuda, T. Hasegawa, A. Ota, H. Yamochi, G. Saito, R. Tazaki, S-I. Adachi, S-Y. Koshihara Science. **307**, 86 (2005).
[8] N. Fukazawa, M. Shimizu, T. Ishikawa, Y. Okimoto, S-Y. Koshihara, T. Hiramatsu, Y. Nakano, H. Yamochi, G. Saito, and K. Onda, J. Phys. Chem. C **116**, 5892 (2012).
[9] K. Onda, H. Yamochi, and S-Y. Koshihara, Acc. Chem. Res. **47**, 3494 (2014).
[10] W.J. Hehre, L. Radom, P.R. Schleyer, and J.A. Pople, *Ab initio* molecular orbital theory, John Wiley, New York (1986).
[11] R. Dovesi, R. Orlando, B. Civalleri, C. Roetti, V.R. Saunders, C.M. Zicovich-Wilson, Z. Kristallogr, Z. Kristallogr. **220**, 571 (2005).
[12] C. Adamo and V. Barone, J. Chem. Phys. **110**, 6158 (1999).
[13] G.J. Linker, P.Th. van Duijnen, P.H.M. van Loosdrecht, and R. Broer, Comp. and Theor. Chem. **1069**, 105 (2015).
[14] G. Thiamová and J. Paldus, Eur. Phys. J. D **46**, 453 (2008).